

Ab initio calculation of spin-polarized low-energy electron diffraction pattern for the systems Fe(001) and Fe(001)- $p(1\times 1)$ O

Stephan Borek,¹ Jürgen Braun,¹ Ján Minár,^{1,2} and Hubert Ebert¹¹*Department Chemie, Ludwig-Maximilians-Universität München, Butenandtstraße 5-13, 81377 München, Germany*²*New Technologies-Research Centre, University of West Bohemia, Univerzitni 8, 306 14 Pilsen, Czech Republic*

(Received 20 May 2015; revised manuscript received 24 July 2015; published 17 August 2015)

The construction of a multichannel vector spin polarimeter requires the development of a detector type, which works as a spin polarizing mirror with high reflectivity and asymmetry properties to guarantee for a high figure of merit. Technical realizations are found by spin-polarized electron scattering from a surface at low energies. A very promising candidate for such a detector suitable material consists of an oxygen passivated iron surface, as for example a Fe(001)- $p(1\times 1)$ O surface. We investigate in detail the electronic structure of this adsorbate system and calculate the corresponding spin-polarized low-energy electron scattering. Our theoretical study is based on the fully relativistic SPRKKR method in the framework of density functional theory. Furthermore, we use the local spin-density approximation in combination with dynamical mean field theory to determine the electronic structure of Fe(001)- $p(1\times 1)$ O and demonstrate that a significant impact of correlation effects occurs in the calculated figure of merit.

DOI: [10.1103/PhysRevB.92.075126](https://doi.org/10.1103/PhysRevB.92.075126)

PACS number(s): 71.15.Mb, 85.70.Ay, 75.70.-i, 68.49.Jk

I. INTRODUCTION

The first quantitative theoretical description of relativistic spin-polarized low-energy electron diffraction (SPLEED) had been developed by Feder [1] and by Tamura and Feder [2]. The advantage of a spin-polarized relativistic formulation consists in the fact that the interplay of exchange interaction and spin-orbit coupling is considered on the same level of accuracy [3,4]. The application of this method to electron scattering from solid surfaces allows one to support the development of a multichannel vector spin polarimeter which can be realized using selected surfaces as two-dimensional reflection mirrors. The concept of such a detection method using spin-dependent electron scattering has been demonstrated, for example, for W(100) [5]. While in the cited work the detection of only one spin component has been realized the new scattering mirror should give the possibility to detect all three spin components in a single step. Therefore, an optimization of suitable materials for use as reflection mirrors and corresponding investigations of new materials is highly desirable. The actual research activities focus on two classes of single crystal surfaces: nonmagnetic surfaces from high- Z materials, where spin-orbit coupling acts as the underlying physical mechanism or magnetic surfaces (ferromagnetic materials) where both exchange interaction and spin-orbit coupling influence the spin-dependent electron scattering. The classical system representing the spin-orbit case is W(100) [6]. Another promising candidate was found in the Ir(001) surface, which is less reactive than tungsten and, as a consequence, provides a longer operation time for use as a spin detector [7]. In contrast the scattering at ferromagnetic surfaces has been investigated only recently [8]. Nevertheless, it was shown that by using ferromagnetic materials as spin detectors a very high figure of merit (FOM) can be achieved [9].

In past decades significant theoretical and experimental progress was made in the application of such systems. One major success of these investigations was the determination of surface magnetic moments [4]. For the exchange scattering of electrons from a sample surface different ferromagnetic

materials have been used [8,10–12]. An often mentioned problem of spin detectors which depend on spin-orbit interaction is the low FOM in the order of 10^{-4} [7]. A higher FOM was reported for exchange scattering from an iron surface where values up to 20 times larger have been reached [8,10–12]. A disadvantage of these surfaces is their short operation time due to contamination. A solution to this problem is the preparation of an oxygen overlayer, i.e., a surface passivation. For the coverage of one monolayer oxygen an ordered overlayer is formed resulting in $p(1\times 1)$ LEED reflection patterns, leading therefore to a longer operation time in vacuum [10]. In this theoretical study the Fe(001)- $p(1\times 1)$ O surface serves as a benchmark for further developments of our theoretical approach, as well as a suitable starting point for research activities on various materials which may be applicable as reflection mirrors for spin filtering.

The paper is organized as follows: In Sec. II we describe the theory of our SPLEED calculations. In Sec. III we discuss our theoretical method concerning the electronic structure and the various SPLEED calculations and in Sec. IV we summarize our results.

II. THEORY

A. Electronic structure

The calculation of the electronic structure has been done using the Munich SPRKKR program package [13–16]. The implementation of the tight-binding (TB) Korringa-Kohn-Rostoker (KKR) method allows an effective treatment of two-dimensional surfaces, i.e., the self-consistent calculation of the electronic structure, due to the fast convergence of the TB structure constants [4,13,14,17–19]. These decay exponentially which allows, in particular, the treatment of various layered systems and relaxed surfaces with adsorbed atoms [20]. Using this method we construct a semi-infinite system with two-dimensional periodicity which consists of three parts: substrate (having bulk potential), surface region, and vacuum region (represented by empty spheres). The calculations were

done fully relativistic to treat effects coming from spin-orbit coupling and exchange interaction in a coherent way. To account for many-body effects beyond the local spin-density approximation [21–23] a site diagonal, nonlocal, complex and energy-dependent self-energy Σ determined within the dynamical mean field approach (DMFT) [24,25] has been used. It has been shown that this method is straightforwardly applicable to semi-infinite lattices with lateral translational invariance and an arbitrary number of atoms per unit cell [26,27]. The inclusion of many-body effects expressed by the DMFT has been shown to result in significant changes for the shape of the calculated spectra especially for lower kinetic energy of the reflected electrons [27]. An important parameter for various spectroscopic calculations is the work function. We calculated the work function of the two-dimensional (2D) semi-infinity system applying a summation over the Madelung potentials in the interaction zone as described elsewhere [28].

B. Theory of SPLEED

The different asymmetries that characterize a SPLEED spectrum of a ferromagnetic surface are determined by changing the magnetization direction parallel to the surface either in the scattering plane or perpendicular to it. The scattering plane is defined by the wave vector of the incident and the scattered electrons. Besides the change of the magnetization the polarization of the incident electrons has to be changed resulting in four different scattered intensities [2,4]. These are determined by the electron polarization (σ) as well as the direction of the magnetization (μ). It has been shown that mainly two different setups have to be considered concerning the orientation of magnetization and polarization with respect to the scattering plane [2]. For our calculations we used the setup for which both magnetization and polarization are parallel to the scattering plane. If this plane is parallel to a mirror plane the spin-orbit asymmetry vanishes and the scattering of the electrons is only due to exchange interaction [4]. According to symmetry considerations for the scattered electron intensities

$$I_{\mu}^{\sigma} = I_{-\mu}^{-\sigma} \quad (1)$$

holds [2]. For the spin-orbit asymmetry (A_{soc}) defined by [4]

$$A_{\text{soc}} = \frac{1}{2}(A_{+} - A_{-}) \quad (2)$$

with the definition for A_{+} and A_{-} ,

$$A_{+} = \frac{I_{+}^{+} - I_{+}^{-}}{I_{+}^{+} + I_{+}^{-}}, \quad (3)$$

$$A_{-} = \frac{I_{-}^{+} - I_{-}^{-}}{I_{-}^{+} + I_{-}^{-}}. \quad (4)$$

$A_{\text{soc}} = 0$ results. The exchange asymmetry (A_{ex}) in turn can be expressed by [4]

$$A_{\text{ex}} = \frac{1}{2}(A_{+} + A_{-}). \quad (5)$$

Based on the symmetry restriction in Eq. (1) one can evaluate A_{ex} from the following simplified equation:

$$A_{\text{ex}} = \frac{I_{+}^{+} - I_{+}^{-}}{I_{+}^{+} + I_{+}^{-}}. \quad (6)$$

As a consequence, the scattering plane is parallel to a mirror plane and only one magnetization direction has to be considered when determining the exchange asymmetry. Nevertheless a useful test is to consider in addition the reversed magnetization to verify vanishing spin-orbit asymmetry.

Another quantity to characterize different working points or regimes for surfaces used as scattering mirror is the FOM. It is defined as the product of the reflected intensity and the asymmetry for a specific orientation of the magnetization:

$$\text{FOM}_{+(-)} = I_{+(-)} A_{+(-)}^2. \quad (7)$$

Here the indices indicate the magnetization direction of the sample. For the use as a spin filter both reflectivity and asymmetry should have high values, leading to a high FOM.

III. DISCUSSION

A. Electronic structure calculation

The calculation of the electronic structure has been started from a fully relaxed surface and interface using experimental structure parameters [29]. For surface sensitive methods it is important to include the structural relaxation of the topmost surface layers. Especially for methods using low energetic particles the changes in the electronic structure resulting from the relaxations are important. We set up a two-dimensional surface system which consists of 10 monolayers (ML) Fe, 1 ML O, and 9 ML empty spheres to simulate the vacuum. In terms of the TB-KKR for 2D systems we introduce left and right bulk regions representing the properties of the Fe substrate and the vacuum. For the left bulk region we used 2 ML of Fe repeated to the left, while 2 ML of the topmost empty spheres have been used for simulating the right bulk region, i.e., the vacuum region. Considering the electronic structure the interaction zone in between simulates the transition from Fe bulk to surface properties. Our calculations were done in the atomic sphere approximation using the parametrization for the exchange-correlation functional of Vosko *et al.* [30]. We used a lattice constant of 2.86 Å according to the unit cell of bcc Fe. A fully relativistic *ab initio* calculation of the potentials was applied to account for spin-orbit and exchange effects on one footing. We also included many-body effects in our calculations considering the sensitivity for spectroscopies based on low energetic particles. For solving the many-body effective impurity problem a DMFT solver has been used [31,32]. In our calculations we utilized the spin-polarized T -matrix approximation solver (TMA) [33]. It has been shown that the use of a TMA solver is justified because of the less pronounced correlation effects in transition metals [34]. The parameters which have to be supplied for a DMFT calculation is the intra-atomic Hund exchange interaction (J) and the screened Coulomb interaction (U). Corresponding to previous extensive studies we set the values to $J = 0.9$ eV and $U = 2.3$ eV [34].

The results of the electronic structure calculations are shown in Fig. 1 in terms of the density of states (DOS) of the first three Fe layers and the O layer. Besides the result of local-density approximation (LDA) calculation the DOS of a DMFT calculation is shown as well.

The DOS shows reasonable agreement with previous electronic structure calculations for the system Fe(001)- $p(1 \times 1)$ O

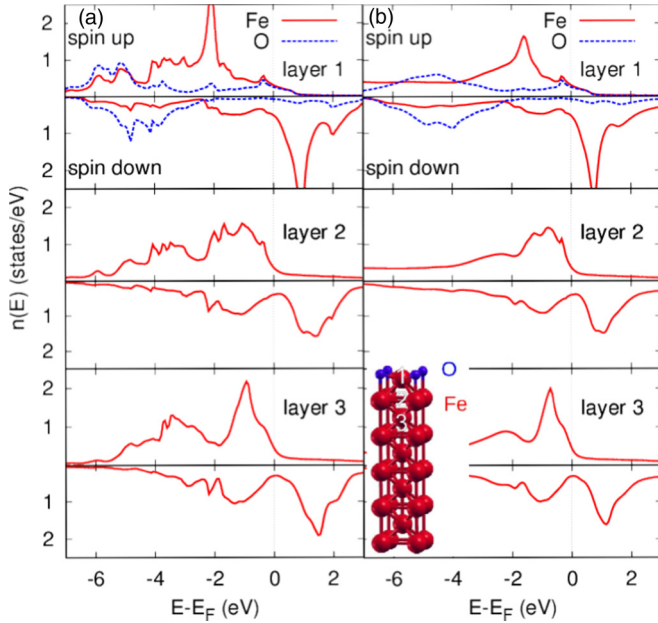


FIG. 1. (Color online) DOS of the first three atomic layers of the investigated half-infinity surface system Fe(001)- $p(1 \times 1)$ O. In (a) the DOS for a standard LSDA calculation is shown. In (b) the calculation includes many-body effects accounting via LSDA + DMFT. The DOS of O and the first Fe layer are drawn together in the uppermost panel to show the hybridization of O and Fe in the valence band. The inset shows a sketch of the surface system and the numbering of the atomic layers.

[35]. It is visible that in the energy regimes -6 eV to -2 eV a hybridization of the valence states between O and the Fe layer occurs. The LSDA + DMFT-based DOS calculations show a broadening especially for the topmost Fe layers resulting in spectral changes for surface sensitive spectroscopic methods. This is caused by the finite value of the self-energy in the specific energy range and is also visible in the calculated band structure (see Figs. 8 and 9). The changes in both spin channels result in a lower spin magnetic moment (m_{spin}) for the DMFT calculations. The main features agree using local spin-density approximation (LSDA) or LSDA + DMFT indicating that the main properties of the electronic and magnetic structure of the Fe(001)- $p(1 \times 1)$ O surface can be described using both schemes. Nevertheless, for the calculation of very low-energy electron diffraction it is important to include LSDA + DMFT (see below). In Fig. 2 the spin and orbital magnetic moments for bcc Fe bulk and the three topmost atomic layers of Fe(001)- $p(1 \times 1)$ O are shown. The Fe atoms of the topmost layer have a higher magnetic moment when compared to the bulk value. This finding is known for magnetic atoms on surfaces and is related to the band narrowing of the d states [36,37]. The trend for the decrease of the spin magnetic moments going to deeper Fe layers is similar for LSDA and LSDA + DMFT calculations. This behavior is reflected by the comparable main features in the DOS (see Fig. 1) comparing LSDA and LSDA + DMFT.

Due to the hybridization of O and Fe in the valence band regime a magnetic moment for O is induced. The increased magnetic moment of Fe for the surface layer in combination

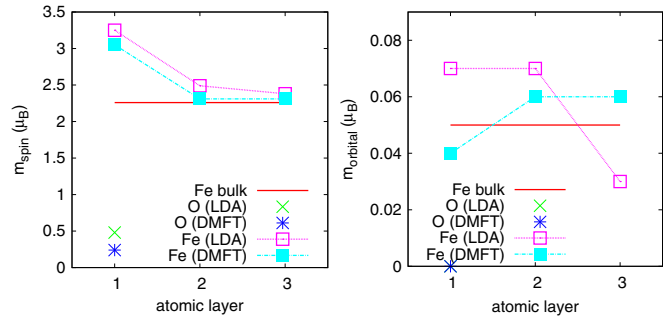


FIG. 2. (Color online) Magnetic moments for Fe bulk and the first three atomic layers of the semi-infinite system Fe(001)- $p(1 \times 1)$ O with and without the inclusion of many-body effects. Besides the spin magnetic moments the orbital moments are shown. For O the orbital moment has zero value for LDA and DMFT.

with the induced magnetic moment for O results in a larger exchange interaction at the passivated Fe(001) surface in contrast to a clean Fe(001) surface. Comparing the spin-orbit-induced orbital magnetic moments the differences between LSDA and LSDA + DMFT calculations are more pronounced than for the spin moments. Using the LSDA an enhancement of the orbital moment for the two outermost atomic layers occurs as one would expect. Besides the decrease of the orbital moment going to deeper Fe layers is stronger for the LSDA calculation. Nevertheless the dominating part is the spin magnetic moment which characterizes the exchange scattering of the polarized electrons. In summary the passivation of the Fe surface results in a significant change of the magnetic properties compared to a nonpassivated Fe surface. In our calculations for the first Fe layer of a nonpassivated Fe surface a spin and orbital magnetic moment $m_s = 2.81\mu_B$ and $m_o = 0.11\mu_B$ results. Whereas for an O passivated surface using the LSDA for the first Fe layer $m_s = 3.25\mu_B$ and $m_o = 0.07\mu_B$ have been calculated. The enlarged magnetic moments result in an increased exchange scattering as has been shown in previous experiments [10]. Also a very high Sherman function was reported which is linked directly to the magnetic properties of the surface [9]. It should be mentioned that our calculated magnetic moments especially for the two surface layers show good agreement with data in the literature [35].

B. SPLEED calculation

For the SPLEED calculations, the scattering plane was aligned along the [100] direction, whereas the surface magnetization as well as the polarization of the electron was aligned along the $[\pm 100]$ direction. All calculations were done for the specularly reflected beam, i.e., the (0,0) beam using the the surface potential barrier of Rundgren-Malmström [38]. For the O passivated Fe(001) surface we calculated a work function of 7.07 eV. In comparison to a clean Fe(001) surface a value of 5 eV was calculated, i.e., an increase of the work function by passivation was found. It should be mentioned that the work function of Fe(001) shows reasonable agreement with experimental and theoretical values in the literature [39]. We calculated polar angle (θ)—energy maps that are shown in Figs. 3–5 for the reflectivity, the exchange asymmetry, and the

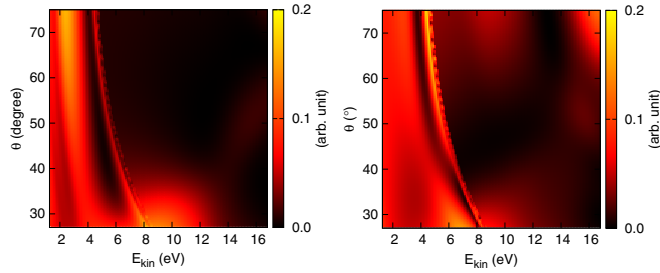


FIG. 3. (Color online) Left: Θ -energy map of the reflectivity for Fe(001). Right: The same for Fe(001)- $p(1 \times 1)$ O.

FOM, respectively. The polar angle was varied in the range from 27° to 75° , whereas the energy range was set to 1.3–17 eV according to the possible working areas as scattering mirror.

In the right panel of Fig. 3 the effective reflectivity of Fe(001)- $p(1 \times 1)$ O is shown. As can be seen we get a huge reflectivity especially for relatively low kinetic energies over the full range of polar angles. In particular, at a kinetic energy of 6 eV and a polar angle of 30° a maximum of the reflectivity occurs. Also visible in Fig. 3 is the emergence threshold starting around 4 eV and a polar angle of 75° and ending at 8 eV and 27° which marks the occurrence of a new beam. It divides the map into mainly two parts of higher and lower reflectivity. This results from the fact that for kinetic energies above the emergence threshold the additional scattering channel lowers the intensity of the specular beam as shown in recent experiments [40]. The left panel in Fig. 3 shows the effective reflectivity for a clean Fe(001) surface. For the passivated Fe surface higher values for kinetic energies greater than the emergence threshold have been obtained. This is due to the higher exchange scattering for the oxygen passivated Fe surface coming out of the higher magnetic moments at the topmost atomic layers.

In Fig. 4 the exchange asymmetry for Fe(001) and Fe(001)- $p(1 \times 1)$ O, respectively, is shown. The plots include different areas according to the preferred reflected spin orientation for a defined orientation of the magnetization.

The positive values of the exchange asymmetry correspond to a parallel alignment of the electron spin and the sample magnetization. For Fe(001)- $p(1 \times 1)$ O in the energy region below the emergence threshold the scattering of parallel aligned electron spin and magnetization is preferred except for a small area located at the emergence threshold. For polar angles larger than 50° a crossing of the emergence threshold results in a

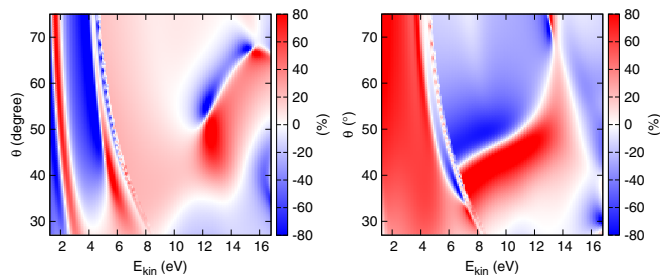


FIG. 4. (Color online) Left: Exchange asymmetry (A_+) for Fe(001). Right: The same for Fe(001)- $p(1 \times 1)$ O.

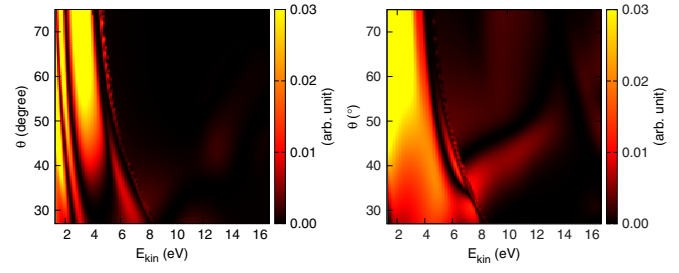


FIG. 5. (Color online) Left: Θ -energy map of the exchange FOM for Fe(001). Right: The same for Fe(001)- $p(1 \times 1)$ O.

change of the scattering behavior. In this case the reflected spin direction can be rotated by changing the kinetic energy of the diffracted electrons. For kinetic energies higher than 6 eV the scattering of electrons with antiparallel spin alignment is preferred. Besides a change of the polarization of the electron a change of the magnitude occurs. The values of the calculated exchange asymmetry fit well to the experimental data [40].

Comparing the results for the asymmetry of Fe(001) and Fe(001)- $p(1 \times 1)$ O one notes that for the complete range of energy and polar angles the asymmetry changes. This is due to the different magnetic properties of the Fe(001) and the Fe(001)- $p(1 \times 1)$ O surfaces. At kinetic energies below the emergence threshold the asymmetry for Fe(001)- $p(1 \times 1)$ O shows broader areas with one specific asymmetry direction. This is in line with other investigations made for these systems [10].

In Fig. 5 the FOM is shown which is the most important observable for characterizing a material to be used as possible spin filter. On the left side the FOM for Fe(001) is shown, whereas on the right side the FOM for Fe(001)- $p(1 \times 1)$ O is shown. For the oxygen passivated surface a broad range of a high FOM for kinetic energies lower than the emergence threshold occurs. This comes from the asymmetry A_+ (see Fig. 4) according to Eq. (7). It is an advantage for the application as spin filter using low kinetic energy electron diffraction for the determination of surface properties. For Fe(001)- $p(1 \times 1)$ O the highest values are reached for kinetic energies lower than 4 eV and a polar angle larger than 50° . Due to the fact that working points for spin filters are suitable between 40° and 60° the oxygen passivated surface is a promising candidate for such an application.

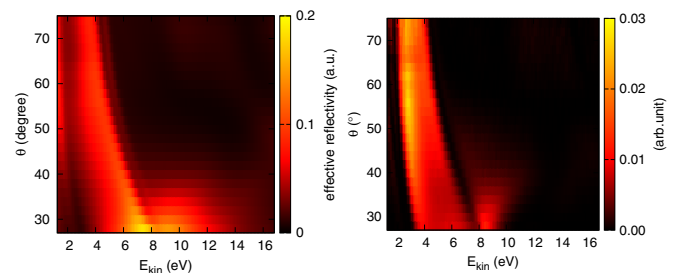


FIG. 6. (Color online) Experimental results for the SPLEED measurements on Fe(100)- $p(1 \times 1)$ O taken from Ref. [40] (reproduced by permission). Left: Θ -energy map of the reflectivity. Right: Θ -energy map of the exchange FOM.

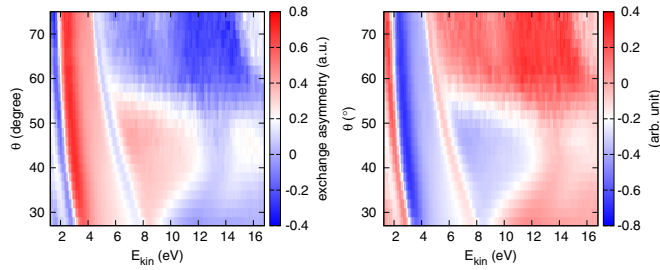


FIG. 7. (Color online) Experimental results for the SPLEED measurements on Fe(100)- $p(1\times 1)$ O taken from Ref. [40] (reproduced by permission). Left: Θ -energy map of the exchange asymmetry. Right: Θ -energy map of the exchange asymmetry for the reversed magnetization.

In Figs. 6 and 7 the experimental results for the reflectivity, the FOM, and the exchange asymmetry are shown for comparison [40].

The emergence threshold is well reproduced by the theoretical results, i.e., its correspondence for varying polar angle and kinetic energy. Hence the geometric configuration described by our calculations match the setup in the experiment. Also the inner potential calculated out of the work function and the Fermi energy is confirmed. This is ensured by the fact that a difference to the experiment would result in an energy shift of the emergence threshold. In Fig. 7 the change of the exchange asymmetry is shown by reversing the magnetization of the Fe(100)- $p(1\times 1)$ O surface. The same behavior as in the theoretical results is visible coming out of vanishing spin-orbit asymmetry. Based on that changing the magnetization direction exactly inverses the scattered polarization of the electrons.

C. Many-body effects in SPLEED calculations

The importance of the inclusion of many-body effects for spectroscopic calculations has been shown in different works [26,27,41–43]. Because of the low kinetic energy of the incident electrons many-body effects might become important for the spectroscopic calculations due to changes of relevant bands (surface states, bands at the Fermi energy, unoccupied states) resulting from a change of the underlying electronic structure calculations. In Fig. 8 the band structure of Fe(001)- $p(1\times 1)$ O with and without inclusion of the DMFT is shown. As one notes, the bands around 7 eV above the Fermi level are smeared out by many-body interactions. This

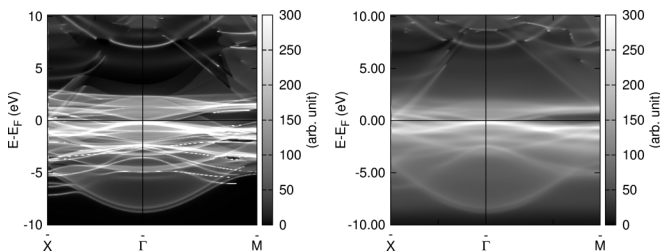


FIG. 8. Left: Bloch spectral function without consideration of many-body effects for Fe(001)- $p(1\times 1)$ O. Right: Results including many-body effects via the DMFT for Fe(001)- $p(1\times 1)$ O.

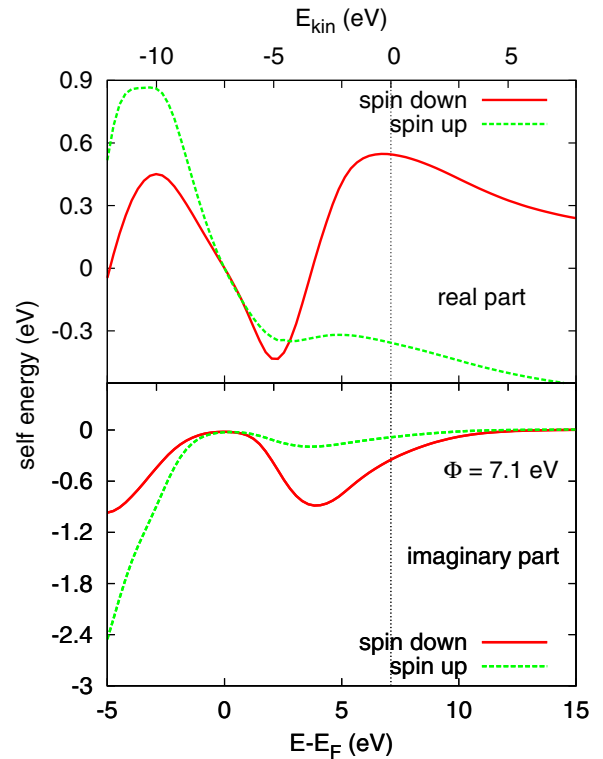


FIG. 9. (Color online) Real and imaginary parts of the self-energy for both spin channels.

energy range is important for SPLEED giving characteristic spectral features. Changes in the band dispersion results in different magnetic properties altering the exchange interaction at the sample surface. This effect can be connected to the self-energy shown in Fig. 9. Comparing to the calculated work function (7.07 eV) the self-energy has a nonzero value affecting the valence bands relevant for the exchange scattering process. Although our calculations show that the impact on the effective reflectivity and the exchange asymmetry is negligible, the changes in the FOM are significant.

In Fig. 10 we present the FOM for Fe(001)- $p(1\times 1)$ O resulting from LSDA + DMFT-based SPLEED calculations. Additionally we considered the change in the projection of the polarization of the electron concerning the surface when changing the polar angle. In comparison to Fig. 5 this results in a shift of the maximal value of the FOM to a polar angle

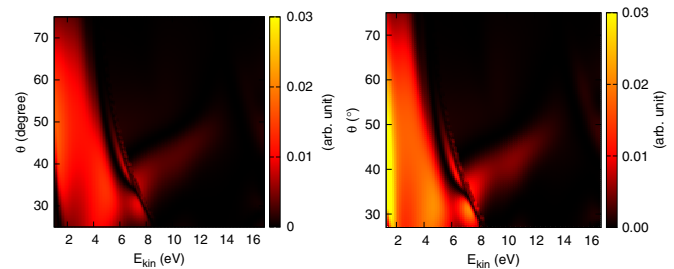


FIG. 10. (Color online) FOM without (left) and with (right) consideration of many-body effects for Fe(001)- $p(1\times 1)$ O. In both cases the projection of the electron spin has been included.

around 50° . According to the changes of the band structure which affects essentially the band near the Fermi level, changes in the FOM are seen mainly for low kinetic energies. This is important comparing measurements and calculations of spectra for low-energy electron diffraction.

IV. SUMMARY

We have shown that the calculations done using our *ab initio* method regarding the SPLEED spectra for Fe(001)- $p(1 \times 1)$ O are in satisfying agreement with recent experimental results [40]. Therefore our description of the systems electronic properties seem to be confirmed. The system exhibits a large FOM and various suitable areas for the application as a spin-polarizing mirror. We have shown that a projection of

the polarization of the electron has a huge impact on the exchange scattering, especially for the calculation of the FOM. Furthermore the inclusion of many-body effects has been considered in SPLEED calculations showing that this results in spectral changes important for the regime of very low-energy electron scattering.

ACKNOWLEDGMENTS

We thank the BMBF (05K13WMA), the DFG (FOR 1346), CENTEM PLUS (LO1402), and the COST Action MP 1306 for financial support. We also thank the group of Professor M. Donath at the Westfälische Wilhelms-Universität Münster for fruitful discussions and for the permission to include the experimental results (all taken from Ref. [40]).

-
- [1] R. Feder, S. F. Alvarado, E. Tamura, and E. Kisker, *Surf. Sci.* **127**, 83 (1983).
- [2] E. Tamura, B. Ackermann, and R. Feder, *J. Phys. C: Solid State Phys.* **17**, 5455 (1984).
- [3] R. J. Celotta, D. T. Pierce, G. C. Wang, S. D. Bader, and G. P. Felcher, *Phys. Rev. Lett.* **43**, 728 (1979).
- [4] R. Feder, *J. Phys. C: Solid State Phys.* **14**, 2049 (1981).
- [5] M. Kolbe, P. Lushchik, B. Peterleit, H. J. Elmers, G. Schönhense, A. Oelsner, C. Tusche, and J. Kirschner, *Phys. Rev. Lett.* **107**, 207601 (2011).
- [6] J. Kirschner and R. Feder, *Phys. Rev. Lett.* **42**, 1008 (1979).
- [7] D. Kutnyakhov, P. Lushchik, A. Fognini, D. Perriard, M. Kolbe, K. Medjanik, E. Fedchenko, S. A. Nepijko, H. J. Elmers, G. Salvatella, C. Stieger, R. Gort, T. Bähler, T. Michlmayer, Y. Acremann, A. Vaterlaus, F. Giebels, H. Gollisch, R. Feder, C. Tusche, A. Krasnyuk, J. Kirschner, and G. Schönhense, *Ultramicroscopy* **130**, 63 (2013).
- [8] F. U. Hillebrecht, R. M. Jungblut, L. Wiebusch, C. Roth, H. B. Rose, D. Knabben, C. Bethke, N. B. Weber, S. Manderla, U. Rosowski, and E. Kisker, *Rev. Sci. Instrum.* **73**, 1229 (2002).
- [9] R. Bertacco, D. Onofrio, and F. Ciccacci, *Rev. Sci. Instrum.* **70**, 3572 (1999).
- [10] R. Bertacco, M. Merano, and F. Ciccacci, *Appl. Phys. Lett.* **72**, 2050 (1998).
- [11] A. Winkelmann, D. Hartung, H. Engelhard, C.-T. Chiang, and J. Kirschner, *Rev. Sci. Instrum.* **79**, 083303 (2008).
- [12] T. Okuda, Y. Takeichi, Y. Maeda, A. Harasawa, I. Matsuda, T. Kinoshita, and A. Kakizaki, *Rev. Sci. Instrum.* **79**, 123117 (2008).
- [13] J. Koringa, *Physica* **13**, 392 (1947).
- [14] W. Kohn and N. Rostoker, *Phys. Rev.* **94**, 1111 (1954).
- [15] H. Ebert, D. Ködderitzsch, and J. Minár, *Rep. Prog. Phys.* **74**, 096501 (2011).
- [16] H. Ebert *et al.*, *The Munich SPR-KKR package*, version 6.3, <http://olymp.cup.uni-muenchen.de/ak/ebert/SPRKKR>, 2012.
- [17] K. Kambe, *Z. Naturforsch.* **22a**, 322 (1967).
- [18] H. Ebert and B. L. Gyorffy, *J. Phys. F: Met. Phys.* **18**, 451 (1988).
- [19] S. C. Lovatt, B. L. Gyorffy, and G.-Y. Guo, *J. Phys. C: Solid State Phys.* **5**, 8005 (1993).
- [20] R. Zeller, P. H. Dederichs, B. Újfalussy, L. Szunyogh, and P. Weinberger, *Phys. Rev. B* **52**, 8807 (1995).
- [21] P. Hohenberg and W. Kohn, *Phys. Rev.* **136**, B864 (1964).
- [22] W. Kohn and L. J. Sham, *Phys. Rev.* **140**, A1133 (1965).
- [23] L. J. Sham and W. Kohn, *Phys. Rev.* **145**, 561 (1966).
- [24] G. Kotliar and D. Vollhardt, *Phys. Today* **57**, 53 (2004).
- [25] A. Georges, *Rev. Mod. Phys.* **68**, 13 (1996).
- [26] J. Minar, L. Chioncel, A. Perlov, H. Ebert, M. I. Katsnelson, and A. I. Lichtenstein, *Phys. Rev. B* **72**, 045125 (2005).
- [27] J. Braun, J. Minar, H. Ebert, M. I. Katsnelson, and A. I. Lichtenstein, *Phys. Rev. Lett.* **97**, 227601 (2006).
- [28] J. Zabloudil, R. Hammerling, L. Szunyogh, and P. Weinberger, *Electronic Scattering in Solid Matter* (Springer-Verlag, Berlin, Heidelberg, 2005).
- [29] S. R. Chubb and W. E. Pickett, *Solid State Commun.* **62**, 19 (1987).
- [30] S. Vosko, L. Wilk, and M. Nusair, *Can. J. Phys.* **58**, 1200 (1980).
- [31] G. Kotliar, S. Y. Savrasov, K. Haule, V. S. Oudovenko, O. Parcollet, and C. A. Marianetti, *Rev. Mod. Phys.* **78**, 865 (2006).
- [32] K. Held, *Adv. Phys.* **56**, 829 (2007).
- [33] S. Chadov, Ph.D. thesis, Universität München, 2007.
- [34] O. Šipr, J. Minár, A. Scherz, H. Wende, and H. Ebert, *Phys. Rev. B* **84**, 115102 (2011).
- [35] A. Tange, C. L. Gao, B. Y. Yavorsky, I. V. Maznichenko, C. Etz, A. Ernst, W. Hergert, I. Mertig, W. Wulfhekkel, and J. Kirschner, *Phys. Rev. B* **81**, 195410 (2010).
- [36] E. Tamura, R. Feder, G. Waller, and U. Gradmann, *Phys. Status Solidi B* **157**, 627 (1990).
- [37] C. L. Fu and A. J. Freeman, *J. Magn. Mater.* **69**, L1 (1987).
- [38] J. Rundgren and G. Malmström, *J. Phys. C: Solid State Phys.* **10**, 4671 (1977).
- [39] H. L. Skriver and N. M. Rosengaard, *Phys. Rev. B* **45**, 9410 (1992).
- [40] C. Thiede, C. Langenkämper, K. Shirai, A. B. Schmidt, T. Okuda, and M. Donath, *Phys. Rev. Appl.* **1**, 054003 (2014).
- [41] K. Haule and G. Kotliar, *Physica B* **359–361**, 139 (2005).
- [42] I. Di Marco, P. Thunström, M. I. Katsnelson, J. Sadowski, K. Karlsson, S. Lebègue, J. Kanski, and O. Eriksson, *Nat. Commun.* **4**, 2645 (2013).
- [43] A. X. Gray, C. Papp, S. Ueda, B. Balke, Y. Yamashita, L. Plucinski, J. Minar, J. Braun, E. R. Ylvisaker, C. M. Schneider, W. E. Pickett, H. Ebert, K. Kobayashi, and C. S. Fadley, *Nat. Mater.* **10**, 759 (2010).